ISSN1027-5495. Functional Materials, 31, No.1 (2024), p. 119-127
doi:http://dx.doi.org/10.15407/fm31.01.119

Q-factor of plasmonic resonances and field enhancement in the vicinity of spherical metallic nanoparticles

A.V. Korotun[1,2], H.V. Moroz[1], R.Yu. Korolkov[1]

[1] National University Zaporizhzhia Polytechnic б,
64 Zhukovsky Str., Zaporizhzhia, 69063, Ukraine
[2] G.V. Kurdyumov Institute for Metal Physics of National Academy of Sciences of Ukraine, 36 Academician Vernadsky Blvd., Kyiv, 03142, Ukraine

Received November 11, 2023

This work investigates the optical response of spherical metal nanoparticles under scattering and absorption conditions, as well as the field enhancement in the vicinity of the nanoparticles due to the excitation of surface plasmon resonance. Relations are obtained to determine the frequency dependence of the field enhancement and the size and frequency dependence of Q-factor, taking into account all relaxation mechanisms. The radii of spherical particles of different metals, at which the surface and radiation relaxations make the same contribution into the effective relaxation rate, as well as the radii at which the effective relaxation rate will be minimal, have been estimated. It has been shown that a decrease in the linewidth of the surface plasmon resonance leads to an increase both in Q-factor and in the magnitude of the field enhancement in the vicinity of nanoparticles..
Keywords: spherical metallic nanoparticle, surface plasmonic resonance, Q-factor, field enhancement, effective relaxation rate, Drude model.

Добротність плазмонних резонансів та підсилення полів в околі сферичної металевої наночастинки *А.В. Коротун, Г.В. Мороз, Р.Ю. Корольков*

В роботі досліджено оптичний відгук сферичних металевих наночастинок з точки зору розсіювання та поглинання, а також такий наслідок збудження поверхневого плазмонного резонансу як підсилення електричного поля в околі наночастинок. Отримано співвідношення для визначення частотної залежності підсилення полів і розмірної та частотної залежностей добротності з урахуванням усіх механізмів релаксації. Наведено оцінки радіусів сферичних частинок різних металів, за яких внески поверхневої та радіаційної релаксації у ефективну швидкість релаксації є однаковими, а також радіусів, за яких ефективна швидкість релаксації буде мінімальною. Показано, що зменшення ширини лінії поверхневого плазмонного резонансу призводить до зростання як добротності, так і величини підсилення поля в околі наночастинок.

1. Introduction

Nowadays, significant efforts of researchers and practitioners are focused on the development of more sensitive and effective plasmonic hybrid structures for biosensors [1], catalysis [2], photothermal cancer therapy [3,4], controlled drug delivery [5,6], data carriers [7], waveguides [8-10], all-optical switching devices [8].

Optical properties of metallic nanoparticles have been actively studied during last decades. The importance of such studies is that metallic nanoparticles bridge the gap between the properties of an isolated atom and bulk material.

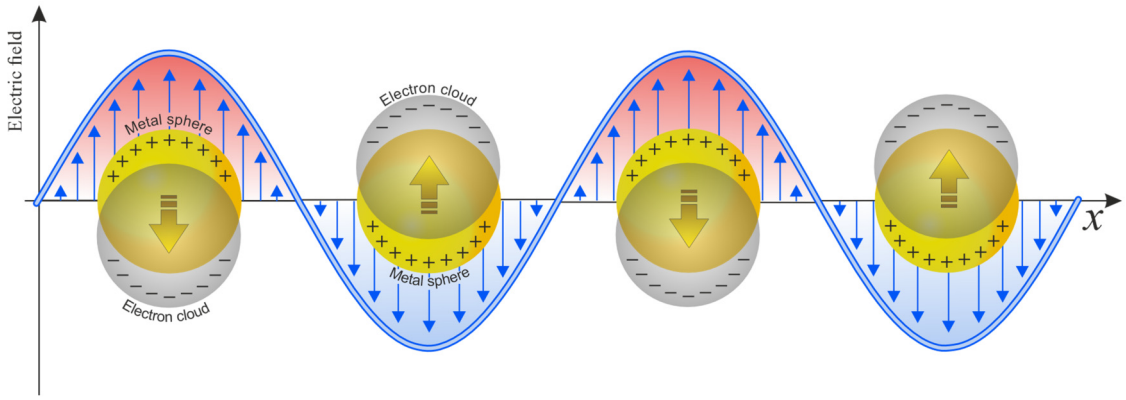

Fig. 1. Scheme of SPR excitation in spherical nanoparticles

The main advantage of noble metals is their unique optical properties, which are determined by the localized surface plasmonic resonance (SPR). The localized SPR is the collective oscillations of conduction electrons at the interface between metallic nanoparticles and their dielectric environment under the excitation by the incident electromagnetic wave. Thus, under the action of an external electromagnetic field, free electrons of metallic nanoparticles begin to oscillate in phase with the electromagnetic field; the frequency of these oscillations is called SPR frequency. The electrical component of the external electromagnetic field induces a force acting on conduction electrons, displacing them from equilibrium positions, and an uncompensated charge is induced on the surface of the particle. The resulting restoring force causes dipole oscillations of all electrons with the same phase. Hence, plasmon can be considered as a harmonic oscillator excited by light. The electron cloud oscillates like a simple dipole parallel to the electric field of electromagnetic radiation (Fig. 1).

The main result of excitation of localized SPR is the strong localization of light energy, which leads to an increase in the electric field near the surface of the particle [11]. The frequency dependence of the electric field enhancement for the spherical bimetallic nanoparticles was described in [12]. The local field enhancement is used in various applications, for example, in surface-enhanced Raman spectroscopy (SERS) [13-15], surface-enhanced fluorescence (SEF) [16], confocal microscopy [17], for increasing the efficiency of solar cells [18] and surface structuring [19].

The optical response of nanostructures is usually studied from the viewpoint of the scattering and absorption. The absorption and scattering spectra of nanoparticles have maxima at the frequencies of localized SPR. At the same time, the optical response is sensitive to morphology, content, size, shape and geometry of the nanostructure [20-22]. An incident electromagnetic wave can be scattered or absorbed depending on the size of the nanoparticle. The absorption process dominates for particles with a diameter less than ~ 50 nm, while for larger particles the main process is scattering. In other words, while large nanoparticles are suitable candidates for the applications requiring strong scattering, small nanoparticles convert absorbed light into heat and act as miniature heat sources [23].

The ability of the plasmonic particles to accumulate energy is characterized by the Q-factor [24, 25]. As a rule, the Q-factor is small ($Q < 10^2$) compared to the values obtained for the dielectric resonators, were the typical values of the Q-factor are 10^5 for Fabry-Perot resonators and up to 10^{11} for the whispering-gallery-mode resonators. For plasmonic particles much smaller than the wavelength, the Q-factor can be calculated in a quasi-static approximation. No matter how the particle shape changes, the Q-factor value cannot exceed this limit value [26]. On the other hand, it is widely accepted that the Q -factor of a particle decreases with increasing particle size, which has been confirmed for spheres and cylinders [27, 28]. At the same time, it was established [29] that the Q-factor is a diagonal tensor for nano-disks of different metals. Moreover, in the vicinity of the SPR frequency, the transverse component of the Q-factor grows with increasing aspect ratio and significantly exceeds the longitudinal component.

The Q-factor is an important criterion which determines both the electromagnetic field en-

hancement [30], and applications associated with the surface-enhanced fluorescence [31]. The shape and sizes of the nanostructures [32] in addition to materials and compositions [33] significantly influence on the characteristics of the surface-enhanced fluorescence. The size of nanoparticles determines the scattering and absorption cross-sections, the location of SPR maximum and the localization of plasmons [33, 34]. Variation of the particle size can increase the fluorescence enhancement coefficient [35]. Controlling and optimizing the fluorescence properties of certain types of materials has led to the widespread use of nanostructures in many fields, from optoelectronics to biological sensing [36, 37].

It should be noted that both radiative and volume-surface loss mechanisms contribute to the damping of collective electron oscillations and, as a consequence, broadening of the localized SPR peak. [38-42]. The radiative mechanism is caused by light re-radiation (scattering) losses and becomes negligible for small spherical metallic nanoparticles, resulting in a narrowing of SPR spectrum [39, 40]. The surface contribution increases and eventually dominates in the broadening of SPR peaks with decreasing particle size, leading to an intrinsic limit to the SPR Q-factor at small particle sizes. Size dependences of SPR frequencies on the shape and size of particles are well known (see, for example, [38]). The width of the SPR line, as believed in a number of experimental [43-46] and theoretical [39, 47-52] works, is a smooth function of the dielectric constant of the medium surrounding the particle. However, in [53, 54] it was proved that the width of the SPR line is an oscillating function of the dielectric permittivity of the matrix.

Thus, a change in the SPR line width leads to a significant change in the frequency dependencies of the Q-factor. This problem has not been previously covered in the scientific literature, so its study is relevant. In view of the above, the aim of the work is to establish a relationship between the size and effective relaxation rate of nanoparticles, and the Q-factor and amplification of electric fields around nanoparticles, taking into account the results of the kinetic approach.

2. Field enhancement near particles

Let a spherical metallic nanoparticle with the radius R is located in a dielectric medium with the permittivity $\epsilon_{\rm m}$ (Fig. 2). The electric

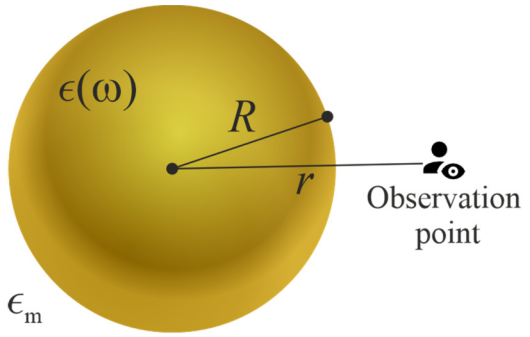

Fig. 2. Geometry of the problem

field enhancement in the vicinity of such a particle is determined by the relation [11]

$$\mathscr{G}(\omega) = \left|1 + \frac{2\alpha(\omega)}{r^3}\right|^2 . \qquad (1)$$

where r is the distance between the center of the nanoparticle and the observation point, and the polarizability is described by the expression

$$\alpha(\omega) = V \frac{\epsilon(\omega) - \epsilon_{\rm m}}{\epsilon(\omega) + 2\epsilon_{\rm m}} . \qquad (2)$$

In formula (2), $V = 4\pi R^3/3$ is the volume of a nanoparticle, and the dielectric function in the Drude model has the form

$$\epsilon(\omega) = \epsilon^{\infty} - \frac{\omega_p^2}{\omega(\omega + {\rm i}\gamma_{\rm eff})} , \qquad (3)$$

where ϵ^{∞} is the contribution of the crystal lattice into the dielectric function; $\omega_p = \sqrt{e^2 n_e / \epsilon_0 m^*}$ is the plasma frequency; e and n_e are the charge and concentration of electrons, correspondingly ($n_e = 3/4\pi r_s^3$; r_s is the mean distance between electrons); ϵ_0 is the vacuum electric constant, and m^* is the effective mass of electrons; ω is the incident light frequency; $\gamma_{\rm eff}$ is the effective relaxation rate, which is determined by the additive contribution of the mechanisms of bulk, surface and radiation attenuation:

$$\gamma_{\rm eff} = \gamma_{\rm bulk} + \gamma_{\rm s} + \gamma_{\rm rad} . \qquad (4)$$

It is known that bulk relaxation rate $\gamma_{\rm bulk} = {\rm const}$ for the particular metal, while the size-frequency dependencies of the surface relaxation rates and radiation attenuation for a spherical metallic nanoparticle have the form [34, 51-54]

$$\gamma_{\rm s} = \frac{1}{4}\left(\frac{\omega_{\rm p}}{\omega}\right)^2 \left[1 - \frac{2\nu_s}{\omega}\sin\frac{\omega}{\nu_s} + \frac{2\nu_s^2}{\omega^2}\left(1 - \cos\frac{\omega}{\nu_s}\right)\right]\frac{v_{\rm F}}{R} , \qquad (5)$$

Table 1. Parameters of metals (see, for example, [34] and the references to them)

Metal	Parameter				
	Z	r_s / a_0	m^* / m_e	ϵ^∞	$\gamma_{\text{bulk}}, 10^{13}\ \text{s}^{-1}$
Al	3	2.07	1.06	0.7	12.5
			1.48		
			1.60		
Cu	1	2.67	1.49	12.03	3.7
	2	2.11			
Au	1	3.01	0.99	9.84	3.45
	3	2.09			
Ag	1	3.02	0.96	3.7	2.50
Pt	2	3.27	0.54	4.42	10.52
Pd	2	4.00	0.37	2.52	13.9

$$\gamma_{\text{rad}} = \frac{1}{24\pi}\frac{V}{\sqrt{\epsilon_{\text{m}}\left(2\epsilon_{\text{m}}+\epsilon^{\infty}\right)}}\left(\frac{\omega_p}{c}\right)^3\left(\frac{\omega_p}{\omega}\right)^2 \times \times\left[1-\frac{2\nu_s}{\omega}\sin\frac{\omega}{\nu_s}+\frac{2\nu_s^2}{\omega^2}\left(1-\cos\frac{\omega}{\nu_s}\right)\right]\frac{\upsilon_{\text{F}}}{R}, \quad (6)$$

where υ_{F} is the speed of Fermi electrons; c is the speed of light; $\nu_s = \upsilon_{\text{F}}/2R$ is the frequency of electron individual oscillations.

The frequency dependence of the Q-factor is determined by the relation

$$Q = \frac{\omega}{2\,\text{Im}\,\epsilon(\omega)}\left(\frac{d\,\text{Re}\,\epsilon(\omega)}{d\omega}\right). \quad (7)$$

We obtain the following expression for the dielectric function, taking into account (3)

$$Q = \frac{\omega_p^2\left(\omega+\gamma_{\text{eff}}\dfrac{d\gamma_{\text{eff}}}{d\omega}\right)}{\gamma_{\text{eff}}\left(\omega^2+\gamma_{\text{eff}}^2\right)}. \quad (8)$$

Further, for convenience, let us represent the expression (4) in the form

$$\gamma_{\text{eff}} = \gamma_{\text{bulk}} + +\mathscr{K}\left(\frac{\omega_p}{\omega}\right)^2\left[1-\frac{2\nu_s}{\omega}\sin\frac{\omega}{\nu_s}+2\left(\frac{\nu_s}{\omega}\right)^2\left(1-\cos\frac{2\nu_s}{\omega}\right)\right]; \quad (9)$$

where

$$\mathscr{K} = \frac{1}{4}\frac{\upsilon_{\text{F}}}{R}\left[1+\frac{V}{6\pi\sqrt{\epsilon_{\text{m}}\left(\epsilon^{\infty}+2\epsilon_{\text{m}}\right)}}\left(\frac{\omega_p}{c}\right)^3\right]. \quad (10)$$

We obtain the following expression from the relation (9)

$$\frac{d\gamma_{\text{eff}}}{d\omega} = 2\mathscr{K}\frac{\omega_p^2}{\omega^3}\left[\frac{4\nu_s}{\omega}\sin\frac{\omega}{\nu_s}+\left(4\left(\frac{\nu_s}{\omega}\right)^2-1\right)\cos\frac{\nu_s}{\omega}-4\left(\frac{\nu_s}{\omega}\right)^2-1\right]. \quad (11)$$

To obtain numerical results, we will use relations (1), (2) and (8) taking into account expressions (3) and (9) – (11).

3. Calculation results and discussion

The frequency dependencies of polarizability and field enhancement and the frequency dependencies of the Q-factor for spherical nanoparticles of different metals in different dielectric media have been calculated. The parameters of metals and dielectrics, required for the calculations, are given in Tables 1 and 2.

It should be noted that the surface scattering dominates in the case of relatively small nanoparticles, while, the radiation attenuation becomes noticeable for the relatively large particles. In this regard, it is of interest to determine the radii R_0 of nanoparticles of various

Table 2. Dielectric permittivities of different matrices [55]

Value	Matrices					
	Air	CaF_2	Teflon	Al_2O_3	TiO_2	C_{60}
ϵ_{m}	1.0	1.54	2.3	3.13	4.0	6.0

Table 3. The radii of nanoparticles at which expression (12) is valid

Metal	R_0, nm			
	Air	CaF_2	Teflon	TiO_2
Au	54.24	59.12	64.39	73.15
Ag	43.40	52.55	58.11	67.47
Cu	40.16	43.70	47.47	53.69
Pt	29.17	32.16	35.46	41.02
Al	25.02	28.43	32.15	38.30

plasmonic metals, for which the radiation attenuation rate and the surface relaxation rate will be equal. From the condition

$$\gamma_s = \gamma_{rad}\,, \tag{12}$$

using (5) and (6) we have

$$R_0 = \frac{c}{\omega_p}\sqrt[3]{\frac{9}{2}\sqrt{\epsilon_m\left(\epsilon^\infty + 2\epsilon_m\right)}}\,. \tag{13}$$

Table 3 shows the calculated values of R_0 for several metals in certain dielectric media. The calculation results show that the value of R_0 decreases in the $Au \to Ag \to Cu \to Pt \to Al$ metal sequence due to an increase in the plasma frequency. At the same time, R_0 increases with increasing permittivity ϵ_m of the environment for particles of the same metal. The effective relaxation rate at the SPR frequency is minimal under the condition

$$\gamma_{eff}(R)\big|_{\omega=\omega_{sp}} \to \min\,. \tag{14}$$

This expression is used to determine the radii of particles of different metals, at which the effective relaxation rate (SPR line width) is minimal, while the field enhancement and the Q-factor are maximal. Since the oscillating terms in (7) and (8) can be neglected compared to unity ($\nu_s \ll \omega$), relation (9) can be rewritten:

$$\gamma_{eff} = \gamma_{bulk} + \mathscr{K}(R)\left(\frac{\omega_p}{\omega}\right)^2, \tag{15}$$

where the expression for $\mathscr{K}(R)$ follows from (10) taking into account $V = 4\pi R^3/3$:

$$\mathscr{K}(R) = \frac{v_F}{4}\left[\frac{1}{R} + \frac{2}{9}\frac{R^2}{6\pi\sqrt{\epsilon_m\left(\epsilon^\infty + 2\epsilon_m\right)}}\left(\frac{\omega_p}{c}\right)^3\right]. \tag{16}$$

In this case, from the minimum condition

$$\frac{d\gamma_{eff}}{dR} = 0$$

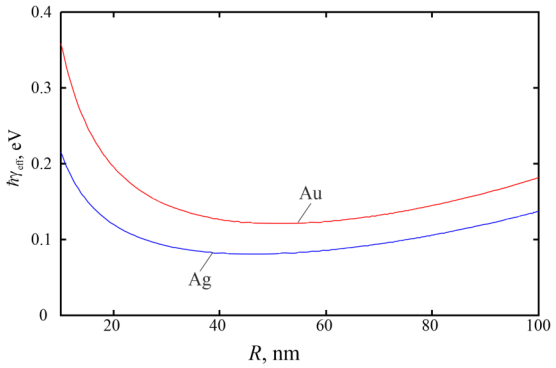

Fig.. 3. Size dependencies of SPR line width for Ag and Au nanoparticles at SPR frequency in Teflon

we obtain

$$R_{min} = \frac{c}{\omega_p}\sqrt[3]{\frac{9}{4}\sqrt{\epsilon_m\left(\epsilon^\infty + 2\epsilon_m\right)}}\,. \tag{17}$$

The comparison of (13) and (17) allows us to obtain the relationship between R_0 and R_{min} in the form:

$$R_{min} = \frac{R_0}{\sqrt[3]{2}}\,. \tag{18}$$

The obtained results are confirmed by the graphs $\gamma_{eff}(R)$ for Au and Ag particles (Fig. 3).

Figure 4 shows the frequency dependencies of the real and imaginary parts and polarizability modulus of spherical Ag nanoparticles of various radii in Teflon. It should be noted that with an increase in the nanoparticle radius, a shift in the minima and maxima $\mathrm{Re}\,\alpha$ and maxima $\mathrm{Im}\,\alpha$, $|\alpha|$ does not occur, while the extrema themselves increase with increasing particle radius, and the width of the SPR line decreases ($\hbar\gamma_{eff}^{(i)}$ in curves 1, 2 and 3 in Fig.4, b). Moreover, there are small-scale oscillations in the graphs $\mathrm{Im}\,\alpha(\hbar\omega)$ with $\hbar\omega < 2.5$ eV, caused by kinetic effects, which manifest themselves in the specified frequency range.

The frequency dependencies of the field enhancement in the vicinity of Ag and Au nanoparticles in Teflon are shown in Figure 5. As in the

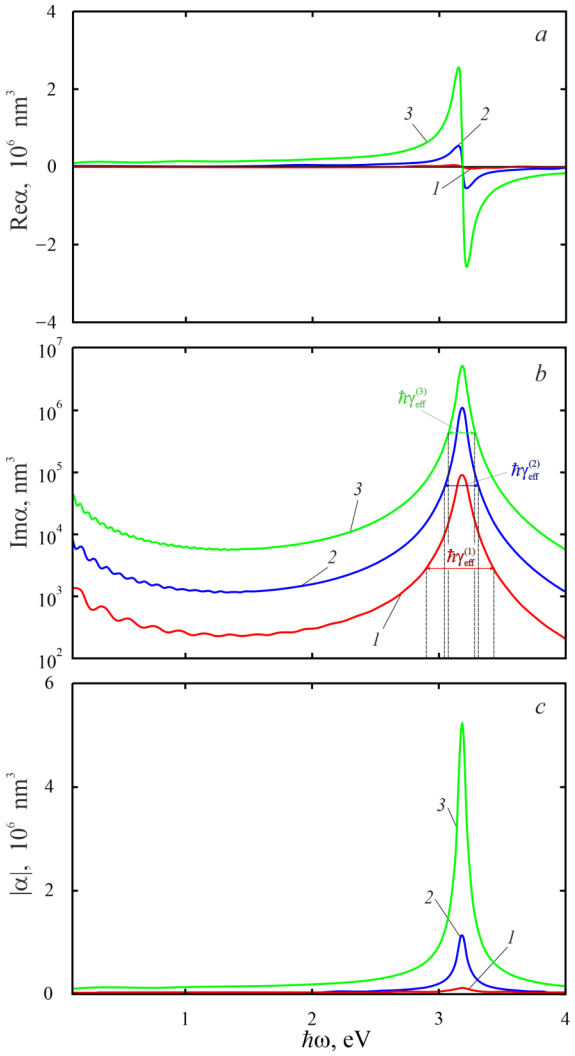

Fig. 4. Frequency dependencies of the real (*a*) and imaginary (*b*) parts, and polarizability modulus (*c*) for spherical Ag nanoparticles in Teflon with various radii: *1* – $R = 15$ nm ; *2* – $R = 30$ nm ; *3* – $R = 50$ nm .

case of polarizability, the enhancement maxima do not shift, and the enhancement reaches its highest values at the nanoparticle boundary. Moreover, the spectral positions $\mathscr{G}_{\max}$ for Ag and Au particles correspond to $\max\{\mathrm{Im}\,\alpha\}$ for these metals.

Figure 6 shows the calculated frequency dependencies of the field enhancement in the vicinity of nanoparticles of different metals in Teflon and in the vicinity of an Ag particle in different dielectrics. The observed "blue" shift $\mathscr{G}_{\max}$ in the $\mathrm{Au} \to \mathrm{Cu} \to \mathrm{Ag} \to \mathrm{Pd} \to \mathrm{Pt} \to \mathrm{Al}$ sequence of metals is explained by the significant difference in the optical properties of these metals, namely, an increase in the plasma frequency ω_p and a decrease in the contribution of interband transitions ϵ^{∞} to the dielectric function. In turn, an increase in the permittivity of the surrounding dielectric leads to a "red" shift of the enhancement maximum. These features of the behavior of the enhancement maxima are fully explained by the dependence of the SPR frequency on the dielectric constant of the matrix, which in the non-dissipative approximation has the following form:

$$\omega_{sp} = \frac{\omega_p}{\sqrt{\epsilon^{\infty} + 2\epsilon_{\mathrm{m}}}}. \qquad (19)$$

Figure 7*a* shows frequency dependencies of the enhancement in the vicinity of Au and Cu nano-spheres in Teflon (taking into account different valences). Since an increase in valence leads to an increase in the concentration of conduction electrons, in turn, both the plasma frequency ω_p and the SPR frequency increase. Hence, an increase in valence leads to a "blue" shift of the field enhancement maxima in the vicinity of nanoparticles.

The curves $\mathscr{G}(\hbar\omega)$ for Al nanoparticles in Teflon (Fig. 7, *b*) indicate an indirect possibility of determining the effective mass of electrons in metals from experimental values of the SPR frequency for spherical nanoparticles.

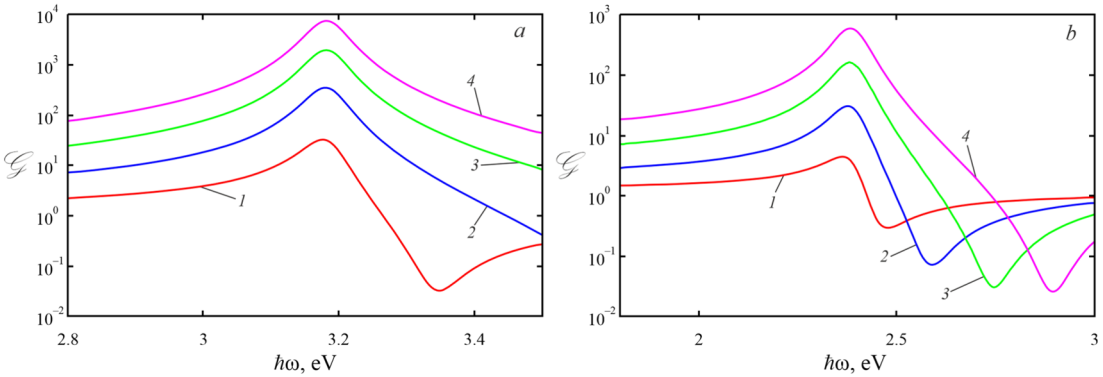

Fig. 5. Frequency dependencies of the field enhancement factor for spherical Ag (*a*) and Au (*b*) nanoparticles of $R = 30$ nm radius in Teflon: *1* – $R/r = 0.4$; *2* – $R/r = 0.6$; *3* – $R/r = 0.8$; *4* – $R/r = 1.0$.

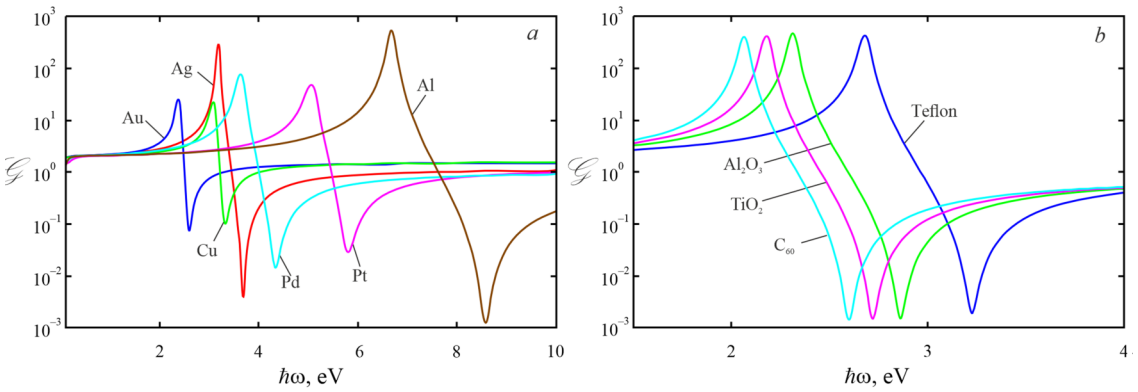

Fig. 6. Frequency dependencies of the field enhancement factor in the vicinity of spherical nanoparticles ($R = 30$ nm ; $R/r = 0.6$) of various metals in Teflon (*a*) and Ag nanoparticles in various media (*b*)

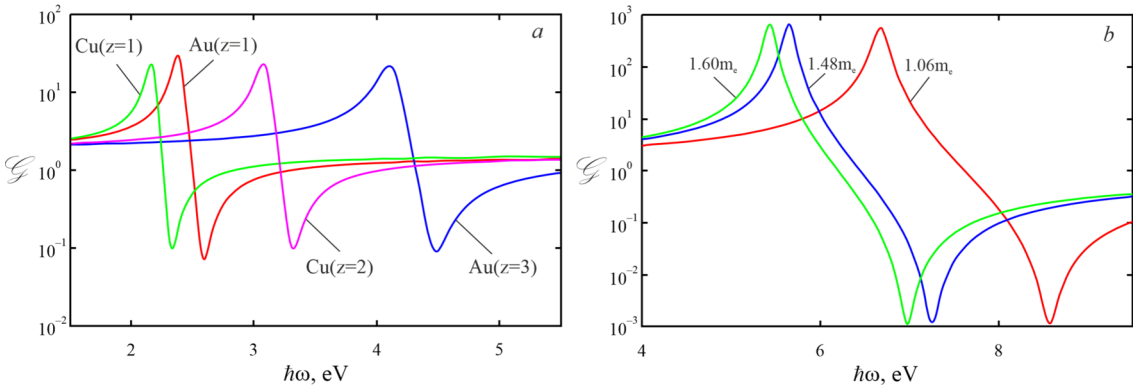

Fig. 7. Frequency dependencies of the field enhancement factor in the vicinity of spherical Au and Cu nanoparticles with different valence (*a*), and Al nanoparticles in Teflon (*b*) with $R = 30$ nm and $R/r = 0.6$

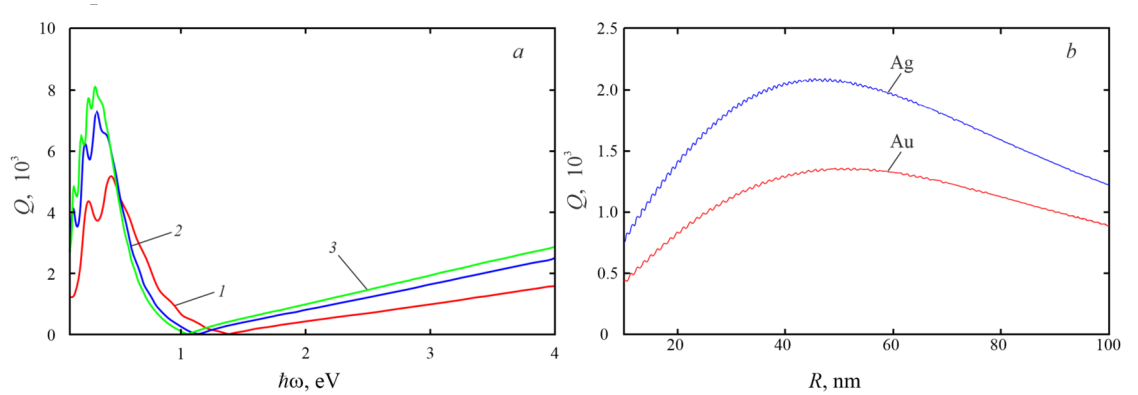

Fig. 8. Frequency dependencies of the Q-factor for spherical Au nanoparticles of different radius (*a*) and the size dependencies of the Q-factor for Ag and Au nanoparticles at SPR frequency (*b*) in Teflon

Figure 8*a* shows the frequency dependencies of the Q-factor for Au nanoparticles of different radii in Teflon. It should be noted that there are noticeable oscillations $Q(\hbar\omega)$ in the near infrared region, at the same time, these oscillations become insignificant at $\hbar\omega > 0.5$ eV. These oscillations are a manifestation of kinetic effects which are significant in the near-infrared region of the spectrum, while in the optical frequency range they practically do not appear [56]. Moreover, in the optical range, the Q-factor increases linearly with increasing frequency; and for any frequency, the Q-factor is greater for the particles of larger radius. This is due to the fact that the calculations are given for the particles with $R < R_0$, where the surface scattering predominates and the Q-factor grows with increasing particle radius.

Figure 8*b* shows the size dependencies of the Q-factor at the SPR frequency for the Ag and Au nanoparticles in Teflon. Note, that the maximum Q-factor corresponds to the minimum of the effective relaxation rate and is achieved under the condition (14). The maxima of $Q(R)$ (Fig. 8, *b*) and minima of $\gamma_{\text{eff}}(R)$ (Fig. 3) at $\omega = \omega_{sp}$ for the spherical Au and Ag particles are achieved at $R = R_{\min}$. At the same time, an increase in radius of nanoparticles leads to a decrease in the Q-factor at $R > R_{\min}$ (when radiation attenuation dominates).

4. Conclusions

Relationships are obtained to determine the frequency dependence of polarizability, the field enhancement factor in the vicinity of a metal spherical nanoparticle, and the Q-factor, taking into account the volumetric, surface and radiation attenuation.

It has been established that an increase in radii of nanoparticles leads to an increase in the extreme values of the real and imaginary parts and the polarizability modulus; however, at the same time, the size shift of the SPR frequency is absent.

It has been shown that the frequency dependence of the field enhancement as well as the imaginary part of the polarizability has a single maximum corresponding to the surface plasmonic resonance, and an increase in the radius of nanoparticles does not lead to a spectral shift. In turn, the field enhancement at the nanoparticle-environment interface is maximum.

The calculations of the enhancement in the vicinity of nanoparticles of different metals and silver nanoparticles in different dielectrics show a blue shift of the enhancement maxima in the metal sequence from gold to aluminum, and a red shift of the maxima with increasing environment permittivity. This behavior of the enhancement maxima is explained by the corresponding dependence of the SPR frequency on the metal optical parameters and permittivity of environment.

It has been demonstrated that an increase in valence and a decrease in the effective mass of electron leads to an increase in the SPR frequency due to increasing frequency of bulk plasmons. At the same time, the obtained results indicate the possibility of indirect determination of the effective electron mass from the spectroscopic experiments.

The frequency dependences of the Q-factor contain noticeable oscillations in the infrared range due to kinetic effects, whereas the Q-factor increases almost linearly with increasing frequency in the visible and ultraviolet regions.

It has been proved that the maximum value of the Q-factor at the SPR frequency corresponds to the minimum of the effective relaxation rate. It has been shown that the fact of a decrease in the Q-factor with increasing radius of the spherical nanoparticle, described in the literature, takes place for the particles with the radius larger than the radius corresponding to the minimum of the effective relaxation rate.

References

1. J.R. Mejía-Salazar, O.N. Oliveira, *Chem. Rev.*, **118**, 10617 (2018).
2. M.B. Gawande, A. Goswami, T. Asefa et al., *Chem. Soc. Rev.*, **44**, 7540 (2015).
3. S. Lal, S.E. Clare, N.J. Halas, *Acc. Chem. Res.*, **41**, 1842 (2008).
4. S. Wang, H. Xu, J. Ye, *Phys. Chem. Chem. Phys.*, **16**, 12275 (2014).
5. N. Hadilou, A. Navid-Khoshgenab, M. Amoli-Diva et al., *J. Pharm. Sci.*, **107**, 3123 (2018).
6. M. Amoli-Diva, R. Sadighi-Bonabi, K. Pourghazi et al., *J. Pharm. Sci.*, **107**, 2618 (2018).
7. P. Zijlstra, J.W.M. Chong, M. Gu, *Nature*, **459**, 410 (2009).
8. S.A. Maier, M.L. Brongerma, P.G. Kik et al., *Adv. Mater.*, **13**, 1501 (2001).
9. S.A. Maier, M.L. Brongerma, P.G. Kik et al., *Phys. Rev. B*, **65**, 193408 (2002).
10. S.A. Maier, P.G. Kik, H.A. Atwater et al., *Nat. Mater.* **2**, 229 (2003).
11. K. Tanabe, *J. Phys. Chem. C*, **112**, 15721 (2008).
12. A.V. Korotun, A.O. Koval, V.V. Pogosov, *Ukr. J. Phys.*, **66**, 518 (2021).
13. K. Kneipp, H. Kneipp, I. Itzkan, R.R. et al., *J. Phys. Cond. Mat.*, **14**, R597 (2002).
14. F. Hubenthal, D. Blázquez Sánchez, N. Borg et al., *Appl. Phys. B*, **95**, 351 (2009).
15. E. Le Ru, J. Grand, N. Felidj et al., *J. Phys. Chem.*, **112**, 8117 (2008).
16. A. Bek, R. Jansen, M. Ringler et al., *Nano Let.*, **8**, 485 (2008).
17. M. Alschinger, M. Maniak, F. Stietz et al., *Appl. Phys. B*, **76**, 771 (2003).
18. M. Westphalen, U. Kreibig, J. Rostalski et al., *Sol. Energy Mater Sol. Cells*, **61**, 97 (2000).
19. F. Hubenthal, *Eur. J. Phys.*, **30**, S49 (2009).

20. P.K. Jain, K.S. Lee, I.H. El-Sayed et al., *J. Phys. Chem.*, **110**, 7238 (2006).
21. V. Myroshnychenko, J. Rodríguez-Fernández, I. Pastoriza-Santos et al., *Chem. Soc. Rev.* **37**, 1792 (2008).
22. A.V. Korotun, N.I. Pavlyshche, *Funct. Mater.*, **29**, 567 (2022).
23. G. Baffou, R. Quidant, C. Girard, *Appl. Phys. Lett.* **94**, 153109 (2009).
24. S. Maier, H. Atwater, *J. Appl. Phys.*, **98**, 011101 (2005).
25. P.R. West, S. Ishii, G.V. Naik et al., *Las. Phot. Rev.*, **4**, 795 (2010).
26. F. Wang, Y.R. Shen, *Phys. Rev. Lett.* **97**, 206806 (2006).
27. K. Kolwas, A. Derkachova, *J. Quant. Spectrosc. Radiat. Transf.*, **114**, 45 (2013).
28. J.M. Nápoles-Duarte, M.A. Chavez-Rojo, M.E. Fuentes-Montero et al., *J. Opt.*, **17**, 065003 (2015).
29. N. Pavlyshche, A. Korotun, I. Titov, V. Tretiak, Quality factor of the surface plasmonic resonance in the metallic nanodiscs. *In: 2021 IEEE 12th International Conference on Electronics and Information Technologies (ELIT)*, (2021) p. 228.
30. E.C. Le Ru, P.G. Etchegoin, Introduction to Plasmons and Plasmonics. In Principles of Surface-Enhanced Raman Spectroscopy, Elsevier: Amsterdam, The Netherlands (2009).
31. J.-E. Park, J. Kim, J.-M. Nam, *Chem. Sci.*, **8**, 4696 (2017).
32. P. Strobbia, E. Languirand, B.M. Cullum, *Opt. Eng.* **54**, 100902 (2015).
33. M. Rycenga, C.M. Cobley, J. Zeng et al., *Chem. Rev.*, **111**, 3669 (2011).
34. A.V. Korotun, N.I. Pavlyshche, *Phys. Met. Metal.*, **122**, 941 (2021).
35. M.A. Badshah, J. Ju, X. Lu et al., *Sens. Act. B Chem.*, **274**, 451 (2018).
36. L. Liu, J. Zhang, M.A. Badshah et al., *Sci. Rep.*, **6**, 22445 (2016).
37. M.A. Badshah, J. Kim, H. Jang et al., *Polymers*, **10**, 649 (2018).
38. U. Kreibig, M. Vollmer, Optical properties of metal clusters, Springer Verlag, Berlin (1995).
39. A. Kawabata, R. Kubo. *J. Phys. Soc. Jpn.*, **21**, 1765 (1966).
40. A. Wokaun, J.P. Godon, P.F. Liao, *Phys. Rev. Lett.*, **48**, 957 (1982).
41. T. Klar, M. Perner, S. Grosse et al., *J. Phys. Rev. Lett.*, **80**, 4249 (1998).
42. C. Sonnichsen, T. Franzl, T. Wilk et al., *Phys. Rev. Lett.*, **88**, 077402 (2002).
43. C. Noguez, *J. Phys. Chem. C*, **111**, 3606 (2007).
44. M. Hu, C. Novo, A. Funston et al., *J. Mater. Chem.*, **18**, 1949 (2008).
45. A.Crut, P.Maioli, N. Del Fatti, et al., *Chem. Soc. Rev.*, **43**, 3921 (2014).
46. C.A. Thibodeaux, V. Kulkarni, W.-S. Chang et al., *J. Phys. Chem. B*, **118**, 14056 (2014).
47. B.N.J. Persson, *Surf. Sci.*, **281**, 153 (1993).
48. E.A. Coronado, G.C.Schatz, *J. Chem. Phys.*, **119**, 3926 (2003).
49. P.M. Tomchuk, M.I. Grigorchuk, *Metallofiz. Noveishie Tekhnol.*, **29**, 623 (2007).
50. P. Tuersun, *Optik*, **127**, 250 (2016).
51. N.I. Grigorchuk, P.M. Tomchuk, *Phys. Rev. B*, **84**, 085448 (2011)
52. N.I. Grigorchuk, *EPL*, **97**, 45001 (2012).
53. N.I. Grygorchuk, *Metallofiz. Noveishie Tekhnol.*, **38**, 717 (2016).
54. N.I. Grigorchuk *J. Phys. Stud.*, **20**, 1701-1 (2016).
55. N.A. Smirnova, M.S. Maniuk, A.V. Korotun et al., *Phys. Chem. of Sol. St.*, **24**, 181 (2023).
56. A.V. Korotun, A.A. Koval', V.I. Reva, *J. Appl. Spectrosc.*, **86**, 606 (2019).